



Photo Switching Hot Paper

How to cite: *Angew. Chem. Int. Ed.* **2021**, *60*, 25753–25757

International Edition: doi.org/10.1002/anie.202111493

German Edition: doi.org/10.1002/ange.202111493

Light-Induced On/Off Switching of the Surfactant Character of the *o*-Cobaltabis(dicarbollide) Anion with No Covalent Bond Alteration

Abdelazim M. A. Abdelgawwad, Jewel Ann Maria Xavier, Daniel Roca-Sanjuán, Clara Viñas, Francesc Teixidor,* and Antonio Francés-Monerris*

Abstract: Cobaltabis(dicarbollide) anion (*[o*-COSAN][−]) is a well-known metallacarborane with multiple applications in a variety of fields. In aqueous solution, the *cisoid* rotamer is the most stable disposition in the ground state. The present work provides theoretical evidence on the possibility to photoinduce the rotation from the *cisoid* to the *transoid* rotamer, a conversion that can be reverted when the ground state is repopulated. The non-radiative decay mechanisms proposed in this work are coherent with the lack of fluorescence observed in 3D fluorescence mapping experiments performed on *[o*-COSAN][−] and its derivatives. This phenomenon induced by light has the potential to destruct the vesicles and micelles *cisoid* *[o*-COSAN][−] typically forms in aqueous solution, which could lead to promising applications, particularly in the field of nanomedicine.

The cobaltabis(dicarbollide) anion, [3,3'-Co(1,2-C₂B₉H₁₁)₂][−] abbreviated as *[o*-COSAN][−], is a 3D-aromatic metallabisdicarbollide,^[1] that can be viewed as if two *nido*-[C₂B₉H₁₁]^{2−} units sandwich a Co^{III} atom.^[2] In the last decades, a vast number of studies have described its physical and chemical properties, highlighting its thermal and chemical stability, most probably due to its strong aromatic character.^[2] These and other properties, in conjunction with its facile synthesis^[3] and derivatization,^[2] make this molecule highly attractive for the development of multiple applications in a plethora of fields,^[4,5] including catalysis,^[6,7] redox chemistry,^[8] (bio)sensors,^[9–11] medicine,^[5,12–16] metal-organic frameworks,^[17] conducting polymers,^[18,19] and surfactants,^[20,21] among others.^[5,22]

Recently, Malaspina et al^[20] rationalized the peculiar ability of *[o*-COSAN][−] to form vesicles and micelles in bulk water, finding that the molecule has indeed very well differentiated hydrophobic and hydrophilic regions. The former corresponds to the surface spanned by the four carbon atoms, characterized by a low net charge density, whereas the latter is ascribed to the geometrically opposed boron atoms, that localize the net negative charge of the molecule. *[o*-COSAN][−] exists in three different rotamers, namely *transoid*-*[o*-COSAN][−], *gauche*-*[o*-COSAN][−], and *cisoid*-*[o*-COSAN][−]. Their relative populations in water solution at 298 K, estimated through the Boltzmann thermodynamic equilibrium distribution, are 1.4 %, 12.8 %, and 85.8 %, respectively.^[20] The surfactant properties of *[o*-COSAN][−] in water solution are thus explained by the preference for the *cisoid* rotamer, which orients the four carbon atoms toward the same side of the molecule, generating amphiphilic properties.^[20] Following this reasoning, it is rational to expect that the *transoid* rotamer, in which the two couples of adjacent carbon atoms face opposite sides, will lack these surfactant properties.

This work is thus aimed to find whether light could be used to stabilize, kinetically and/or thermodynamically, other isomers rather than the thermally stable *cisoid* *[o*-COSAN][−] rotamer in aqueous solution. Apart from the fundamental interest in the discovery of novel molecular rotors, as reported for the related Ni^{III} metallabis(dicarbollide),^[23] this hypothesis, if correct, could have potential practical relevance as on/off light switchable surfactants having significant applications in multiple relevant fields, for example, in drug delivery. Nanomedicine often fails to translate efficacies from preclinical trials to clinical administration due to heterogeneity in enhanced permeability and retention in human cancer cells.^[24] A photo-responsive nanocarrier formed by self-assembly of small molecules, *[o*-COSAN][−], wherein each individual molecule is a photo-responsive surfactant, can possibly enhance efficacy in clinical trials.

This hypothesis is motivated by the recent finding of Guerrero et al, which characterized the bright excited state of *[o*-COSAN][−] as an electronic promotion from the carborane skeleton to the cobalt atom (ligand-to-metal charge transfer or LMCT),^[7] and the usual antibonding character of empty *d* orbitals of first-row transition metals, that could elongate the metal-boron coordination bonds, thus diminishing the steric hindrance for the relative rotation of the [C₂B₉H₁₁]^{2−} units, as suggested in a previous work.^[25]

Herein, results are obtained through a combination of density functional theory (DFT),^[26] time-dependent (TD)-DFT,^[26] multiconfigurational complete-active-space second-order perturbation theory (CASPT2) calculations,^[27] and 3D

[*] A. M. A. Abdelgawwad, Dr. A. Francés-Monerris
Departament de Química Física, Universitat de València
46100 Burjassot (Spain)
E-mail: Antonio.Frances@uv.es

J. A. M. Xavier, Prof. Dr. C. Viñas, Prof. Dr. F. Teixidor
Institut de Ciència de Materials de Barcelona, ICMA-B-CSIC
Campus UAB, 08193 Bellaterra (Spain)
E-mail: teixidor@icmab.es

Dr. D. Roca-Sanjuán
Institut de Ciència Molecular, Universitat de València
46071 València (Spain)

Supporting information and the ORCID identification number(s) for the author(s) of this article can be found under:
<https://doi.org/10.1002/anie.202111493>.

© 2021 The Authors. Angewandte Chemie International Edition published by Wiley-VCH GmbH. This is an open access article under the terms of the Creative Commons Attribution Non-Commercial License, which permits use, distribution and reproduction in any medium, provided the original work is properly cited and is not used for commercial purposes.

fluorescence experiments. Full computational details and method validations can be found in the Supporting Information (SI).

The absorption properties of *cisoid*- and *transoid*-[*o*-COSAN][−] are shown in Figure S4. The CASSCF/CASPT2 method describes the most intense absorption in the UV wavelengths as LMCT transitions, confirming previous TD-DFT studies.^[7] CASPT2 determinations predict smaller absorption capacities for *cisoid*-[*o*-COSAN][−] with respect to the *transoid* rotamer. The latter is responsible of the intense band recorded at ≈ 293 nm, whereas the absorption in the visible region (≈ 450 nm) is ascribed solely to triplet absorptions of the *cisoid*-[*o*-COSAN][−]. This result suggests that the presence of *cisoid* and *transoid* rotamers could be tracked at ≈ 450 and ≈ 293 nm, respectively.

Figure 1 displays the photochemical landscape of the *cisoid* and *transoid* rotamers. According to Kasha's rules,^[28] the optically active state populated upon light absorption vibrationally decays to the lowest singlet or triplet excited states via fast internal conversions and intersystem crossing events, also favoured by the high density of states and the large singlet-triplet spin-orbit couplings (SOCs) (see Tables S1–S3 and S5). In both rotamers, optimization of the S₁ state (coordinate 7) elongates all Co–B and Co–C coordination bonds due to the antibonding character of the LMCT state in this region of the molecule (Figure S4). Interestingly, T₁ state relaxation (coordinate 13) is characterized by a further elongation of a Co–C bond and a Co–B connection in *cisoid* [o-COSAN][−] and the two Co–C bonds in *transoid* [o-COSAN][−], while the remaining coordination bond distances decrease. Table S5 lists the bond distances for all rotamers and Figure 1c illustrates the S₁ and T₁ minima stretchings. As shall be discussed below, the increase of the distance between the two [C₂B₉H₁₁]^{2−} units correlates with lower energy rotation barriers between each [o-COSAN][−] rotamers, as compared to those in the ground state.

For [o-COSAN][−], the large SOC between singlet and triplet states (Table S6), typical of molecular systems bearing transition metals,^[29,30] strongly support the population of triplet states during the excited-state relaxation. By inspection of Figure 1, it becomes apparent that the T₁ and T₂ states lie at significantly lower energies with respect to the S₁ surface, indicating that these triplet states will mediate the excited state decay, especially at the T₁ equilibrium structure (coordinate 13). This region is, however, markedly different for both rotamers. Whereas the *cisoid* structure has a T₁–S₀ energy gap of 0.61 eV (14.1 kcal mol^{−1}), the *transoid* isomer displays an energy difference of only 0.21 eV (4.8 kcal mol^{−1}) and can be considered a singlet-triplet crossing (STC) region. Highly accurate CASPT2 results confirm this finding (see Table S7). The potential energy surfaces shown in Figure 1 suggest a longer excited state lifetime for the *cisoid* [o-COSAN][−], as compared to *transoid* [o-COSAN][−], due to the higher energy gap and thus smaller probability of ground-state repopulation via T₁→S₀ intersystem crossing. The predicted longer excited-state lifetime allows the possibility to rotate to the *transoid* arrangement, clearly the most favorable rotamer in the excited state (Figure 2 and Table S8). In the *transoid* arrangement, the non-radiative T₁→S₀ decay is

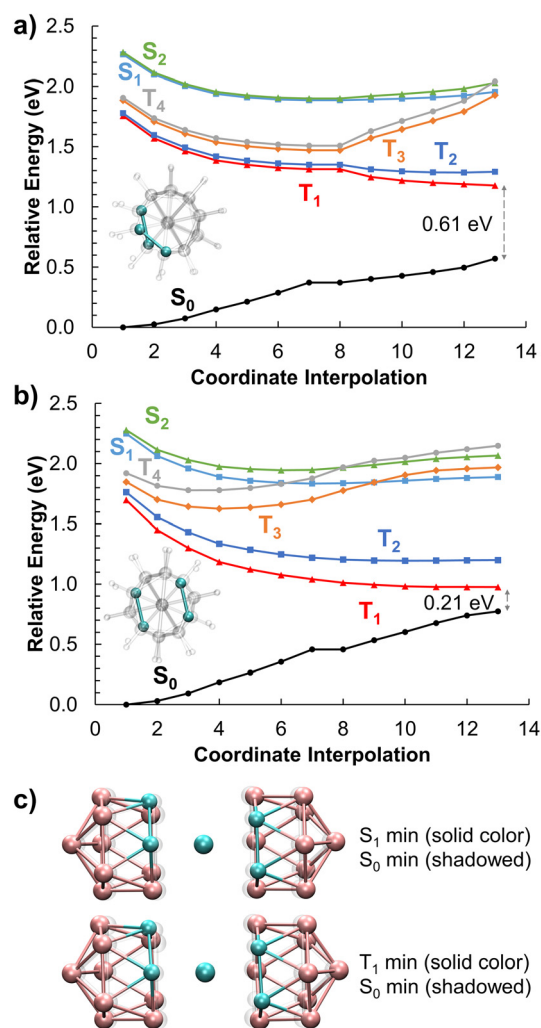


Figure 1. Distinct photophysics of the *cisoid*- (a) and *transoid*-[*o*-COSAN][−] (b) rotamers in water solution. Unrestricted geometry optimizations performed with the B3LYP (S₀ min, coordinate 1) and TD-B3LYP (S₁ and T₁ min, coordinates 7 and 13, respectively) methods. Geometry interpolations have been performed in geodesic coordinates.^[32] Panel (c) compares the S₁ and T₁ minima structures (solid balls and sticks) with the S₀ min geometry (shaded) for *cisoid* [o-COSAN][−]. Hydrogen atoms are not shown.

more efficient, and will be followed by a thermal rotation back to the dominant *cisoid* disposition, the most stable rotamer in the ground state.^[31]

The relative stabilities of the [o-COSAN][−] rotamers in water have been re-assessed in the S₁ and T₁ excited states (see Figure 2). Table S8 compiles the energies both in solution and in the gas phase, at the TD-B3LYP and CASPT2 levels of theory, whereas the dipole moment modules $|\vec{\mu}|$ of each rotamer are compiled in Table S9. In solution, the *gauche* rotamer, intermediate between *cisoid* and *transoid*, is the most stable isomer in the S₁ state. Meanwhile, in the T₁ state, accessible through large singlet-triplet SOC values, the *transoid* rotamer is clearly the most stable rotamer by ≈ 4 kcal mol^{−1}. In the gas phase, the stabilization is even larger (≈ 7 kcal mol^{−1}). This indicates that the photoexcitation of *cisoid*-[o-COSAN][−] in water solution increases the distance

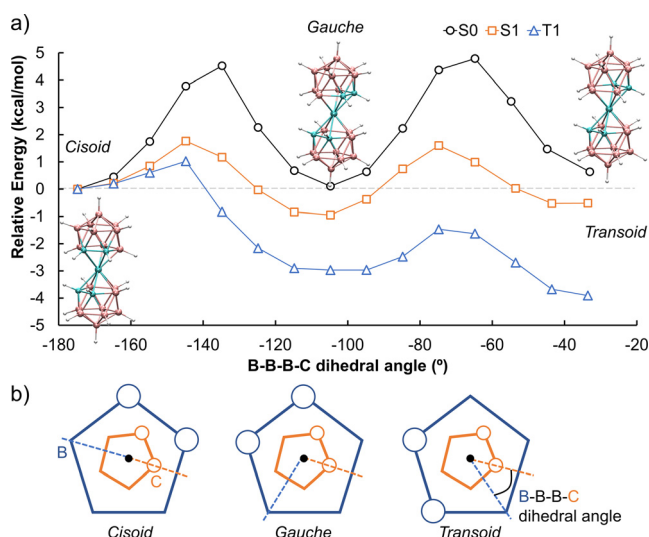


Figure 2. a) S_0 (B3LYP), S_1 and T_1 (TD-B3LYP) relaxed scans of the B-B-B-C dihedral angle in solution. Each curve is relative to the energy of each state at the corresponding *cisoid* structure. Panel (b) describes the B-B-B-C dihedral angle as the angle between the plane defined by the B-B-B atoms (blue dashed lines) and the plane defined by the B-B-C atoms (orange dashed lines), in which the two apical boron atoms (B-B) are shown as a black dot.

between the two $[C_2B_9H_{11}]^{2-}$ ligands, facilitating the rotation of the two units favouring the *transoid* species, thus inducing a *cisoid-to-transoid* photoinduced rotation at a photochemical (fast) scale. To the best of our knowledge, this feature has not been observed until now.

The energy barriers associated to the rotation are reported in Figure 2a. It can be readily seen that the results corroborate the premise made above based on the antibonding character of the orbitals populated upon photoabsorption. Thus, energy barriers of ca. 2 kcal mol^{-1} are obtained for the S_1 and T_1 excited states, while those found for the ground state exceed 4 kcal mol^{-1} . In vacuo, the CASPT2 method (Figure S7c) provides a very similar description to TD-DFT profiles (Figure S7b), even though the *gauche* and *transoid* rotamers are stabilized by $\approx 1 \text{ kcal mol}^{-1}$ in the ground state by the multiconfigurational method. Note that the relative energies between the S_0 , S_1 and T_1 states at each point of the dihedral angle scan cannot be directly compared, since each curve has different energy reference (the energy of each state at the *cisoid* disposition).

The excited-state rotation and decay mechanism are confirmed through state-of-the-art^[33–35] non-adiabatic molecular dynamics^[36,37] performed in a model system, including only the first three singlet and four triplet states in the simulations, initially exciting the S_1 state. Full simulation details can be found in the SI. As expected, populations analysis reveals a fast population of the triplet states within a few hundreds of fs (Figure S9a), with a characteristic time constant for the net triplet population (from both S_1 and S_2 states) that is of 343 fs (Figure S9b), totally coherent with the large singlet-triplet SOCs.

Time evolution of the B-B-B-C dihedral angle (as defined in Figure 2b) reveals that, within our simulation time

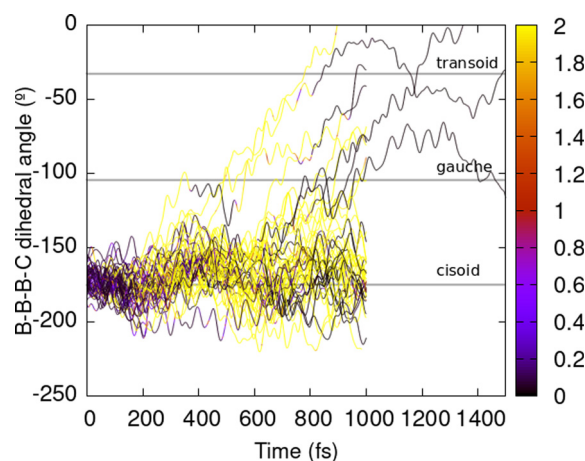


Figure 3. Time evolution of the B-B-B-C dihedral angle of an ensemble of 50 trajectories excited to the S_1 state. The colour code stands for the total spin expectation value $\langle \hat{S}^2 \rangle$, 0 for pure singlet and 2 for pure triplet. The S_0 , S_1 , S_2 , T_1 , T_2 , T_3 , and T_4 states are included in the dynamics.

($\approx 1 \text{ ps}$), $\approx 24\%$ of the molecules undergo a photoinduced rotation (Figure 3). In particular, $\approx 14\%$ reach *gauche* disposition and $\approx 10\%$ already display *transoid* arrangement. Whereas some of the rotations clearly take place in the triplet state, followed by the decay to the ground state when the system reaches the *gauche* or *transoid* regions (as stated above), others occur in the singlet state, even after decay to S_0 , indicating that the triplet state population is not a prerequisite for the photoinduced rotation and that the vibrational excess of energy can also drive the rotation. Meanwhile, this phenomenon is not observed when the dynamics are propagated in the S_0 state (Figure S10), showing the influence of the excited state in inducing the rotation. The most active vibrational normal mode in the excited-state dynamics is characterized by transversal displacements of each carborane cage toward opposite directions (Figures S11–S18).

While the non-adiabatic dynamics performed in this work serve as a proof of concept of the photoinduced rotation and allow an estimation of its yield and timescale, these results shall be considered as a lower bound of the actual rotation properties. More rotations are expected with longer simulation times since the majority of trajectories (64%) remain in the excited state after 1 ps from excitation. On the other hand, only a few excited states are included in the dynamics, while higher energy states can be populated increasing the wavelength range of UV/Vis radiation. The higher excitation energy (and thus vibrational energy) and the presumably longer excited-state lifetimes are expected to increase the rotation yields.

The non-radiative decay mechanisms described in this work, mediated by the population of triplet excited states, explain the absence of luminescence measured for $[o\text{-COSAN}]^-$ in 3D fluorescence experiments. Figure 4a shows the emission spectrum recorded for the sodium salt of $[o\text{-COSAN}]^-$ in aqueous solution, of predominant *cisoid* configuration, irradiated from 300 to 550 nm. No emission signal is detected. The same result is obtained for $[o\text{-COSAN}]^-$ in

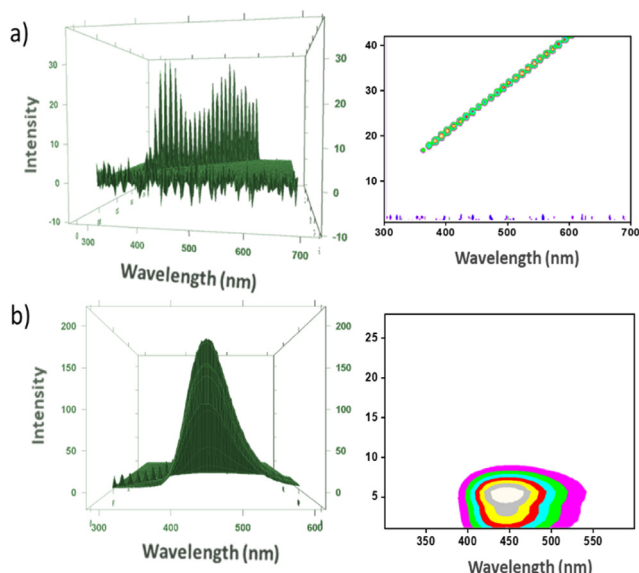


Figure 4. 3D-fluorescence recording of a) Na[o-COSAN] in aqueous solution, and b) quinine sulphate in water.

acetone (Figure S24). In contrast, Figure 4b reveals the well-known emission band of quinine sulfate, which serves as a control experiment in this work. Similar to [o-COSAN]⁻, some of its methyl, phenyl, and chlorinated derivatives, of predominant *transoid* disposition due to the presence of the bulky substituents and/or lone pairs at the substituents, have no emission properties either (Figures S25–S29).

This Communication explores the ability of [o-COSAN]⁻ cluster to constitute a light-induced molecular rotor, a feature that could have consequences in some of its vastly studied properties.^[22] For example, the supramolecular vesicle nanostructures typical of the *cisoid* disposition,^[20] could be disaggregated acting as precisely drug delivery systems under exposition to UV light. Mass spectrum measurements in photocatalysis experiments indicate that [o-COSAN]⁻ is mostly stable upon irradiation.^[7] The present theoretical predictions are also valuable given the experimental difficulties in disentangling the optical and spectroscopic properties of each rotamer. Nonetheless, future experimental set ups able to detect the rotamer population transfers in aqueous solution, for instance through time-resolved spectroscopy, are highly encouraged.

Acknowledgements

This work was supported by the Generalitat Valenciana (GV, project GV/2020/226), Generalitat de Catalunya (2017 SGR 1720), and the Spanish Ministerio de Ciencia e Innovación (MICINN, projects CTQ2017-87054-C2-2-304-P and PID2019-106832RB-I00). A.M.A.A. is grateful to the Erasmus+ Programme of the European Commission for his Erasmus Mundus TCCM scholarship. A.F.-M. is grateful to the GV and the European Social Fund for the postdoctoral contract APOSTD/2019/149 and to the MICINN for the Juan de la Cierva contract IJC2019-039297-I. D.R.-S. is grateful to

the MICINN for the “Ramón y Cajal” grant (RYC-2015–19234). “Severo Ochoa” Program for Centers of Excellence in R&D 234 (SEV-2015-0496) is appreciated. J. A. M. Xavier acknowledges DOC-FAM programme under the Marie Skłodowska-Curie grant agreement No. 754397 and is enrolled in the PhD program of the UAB. Computations have been conducted at the local QCEXVAL and the Lluís Vives and Tirant III clusters of the Servei d’Informàtica (University of Valencia). We thank Dr. Jordi Faraudo (ICMAB-CSIC) for the scientific discussions.

Conflict of Interest

The authors declare no conflict of interest.

Keywords: carborane · quantum chemistry · fluorescence · photodynamics · thermal decay

- [1] J. Poater, C. Viñas, I. Bennour, S. Escayola, M. Solà, F. Teixidor, *J. Am. Chem. Soc.* **2020**, *142*, 9396–9407.
- [2] M. F. Hawthorne, D. C. Young, T. D. Andrews, D. V. Howe, R. L. Pilling, A. D. Pitts, M. Reintjes, L. F. Warren, P. A. Wegner, *J. Am. Chem. Soc.* **1968**, *90*, 879–896.
- [3] I. Bennour, A. M. Cioran, F. Teixidor, C. Viñas, *Green Chem.* **2019**, *21*, 1925–1928.
- [4] J. Plešek, *Chem. Rev.* **1992**, *92*, 269–278.
- [5] N. S. Hosmane, R. D. Eagling, *Handbook Of Boron Science: With Applications In Organometallics Catalysis, Materials And Medicine, Vol. 4*, World Scientific, Singapore, **2018**.
- [6] I. Guerrero, C. Viñas, X. Fontrodona, I. Romero, F. Teixidor, *Inorg. Chem.* **2021**, *60*, 8898–8907.
- [7] I. Guerrero, Z. Kelemen, C. Viñas, I. Romero, F. Teixidor, *Chem. Eur. J.* **2020**, *26*, 5027–5036.
- [8] M. Lupu, A. Zaulet, F. Teixidor, E. Ruiz, C. Viñas, *Chem. Eur. J.* **2015**, *21*, 6888–6897.
- [9] A.-I. Stoica, C. Viñas, F. Teixidor, *Chem. Commun.* **2008**, 6492–6494.
- [10] A.-I. Stoica, C. Viñas, F. Teixidor, *Chem. Commun.* **2009**, 4988–4990.
- [11] D. Kodr, C. P. Yenice, A. Simonova, D. P. Saftić, R. Pohl, V. Sýkorová, M. Ortiz, L. Havran, M. Fojta, Z. J. Lesnikowski, et al., *J. Am. Chem. Soc.* **2021**, *143*, 7124–7134.
- [12] I. Fuentes, T. García-Mendiola, S. Sato, M. Pita, H. Nakamura, E. Lorenzo, F. Teixidor, F. Marques, C. Viñas, *Chem. Eur. J.* **2018**, *24*, 17239–17254.
- [13] E. Hao, M. G. H. Vicente, *Chem. Commun.* **2005**, 1306–1308.
- [14] E. Hey-Hawkins, C. V. Teixidor, *Boron-Based Compounds: Potential and Emerging Applications in Medicine*, Wiley, Hoboken, **2018**.
- [15] P. Cígler, M. Kožíšek, P. Řezáčová, J. Brynda, Z. Otwinowski, J. Pokorná, J. Plešek, B. Grüner, L. Dolečková-Marešová, M. Máša, et al., *Proc. Natl. Acad. Sci.* **2005**, *102*, 15394–15399.
- [16] Y. Zheng, W. Liu, Y. Chen, H. Jiang, H. Yan, I. Kosenko, L. Chekulaeva, I. Sivaev, V. Bregadze, X. Wang, *Organometallics* **2017**, *36*, 3484–3490.
- [17] M. J. Hardie, *J. Chem. Crystallogr.* **2007**, *37*, 69–80.
- [18] C. Masalles, S. Borrás, C. Viñas, F. Teixidor, *Adv. Mater.* **2000**, *12*, 1199–1202.
- [19] R. Núñez, I. Romero, F. Teixidor, C. Viñas, *Chem. Soc. Rev.* **2016**, *45*, 5147–5173.
- [20] D. C. Malaspina, C. Viñas, F. Teixidor, J. Faraudo, *Angew. Chem. Int. Ed.* **2020**, *59*, 3088–3092; *Angew. Chem.* **2020**, *132*, 3112–3116.

- [21] P. Bauduin, S. Prevost, P. Farràs, F. Teixidor, O. Diat, T. Zemb, *Angew. Chem. Int. Ed.* **2011**, *50*, 5298–5300; *Angew. Chem.* **2011**, *123*, 5410–5412.
- [22] B. P. Dash, R. Satapathy, B. R. Swain, C. S. Mahanta, B. B. Jena, N. S. Hosmane, *J. Organomet. Chem.* **2017**, *849–850*, 170–194.
- [23] M. F. Hawthorne, J. I. Zink, J. M. Skelton, M. J. Bayer, C. Liu, E. Livshits, R. Baer, D. Neuhauser, *Science* **2004**, *303*, 1849–1851.
- [24] D. Sun, S. Zhou, W. Gao, *ACS Nano* **2020**, *14*, 12281–12290.
- [25] F. Teixidor, C. Viñas, *Pure Appl. Chem.* **2012**, *84*, 2457–2465.
- [26] Gaussian 16, Revision C.01, M. J. Frisch, G. W. Trucks, H. B. Schlegel, G. E. Scuseria, M. Robb, J. R. Cheeseman, G. Scalmani, V. Barone, G. Petersson, H. Nakatsuji, et al., **2016**, Gaussian, Inc., Wallin.
- [27] I. Fernández Galván, M. Vacher, A. Alavi, C. Angeli, F. Aquilante, J. Autschbach, J. J. Bao, S. I. Bokarev, N. A. Bogdanov, R. K. Carlson, et al., *J. Chem. Theory Comput.* **2019**, *15*, 5925–5964.
- [28] M. Kasha, *Discuss. Faraday Soc.* **1950**, *9*, 14–19.
- [29] M. Gernert, L. Balles-Wolf, F. Kerner, U. Müller, A. Schmiedel, M. Holzapfel, C. M. Marian, J. Pflaum, C. Lambert, A. Steffen, *J. Am. Chem. Soc.* **2020**, *142*, 8897–8909.
- [30] M. Darari, E. Domenichini, A. Francés-Monerris, C. Cebrián, K. Magra, M. Beley, M. Pastore, A. Monari, X. Assfeld, S. Haacke, et al., *Dalton Trans.* **2019**, *48*, 10915–10926.
- [31] E. J. Juárez-Pérez, R. Núñez, C. Viñas, R. Sillanpää, F. Teixidor, *Eur. J. Inorg. Chem.* **2010**, 2385–2392.
- [32] X. Zhu, K. C. Thompson, T. J. Martínez, *J. Chem. Phys.* **2019**, *150*, 164103.
- [33] J. P. Zobel, T. Knoll, L. González, *Chem. Sci.* **2021**, *12*, 10791–10801.
- [34] A. Francés-Monerris, J. Carmona-García, A. U. Acuña, J. Z. Dávalos, C. A. Cuevas, D. E. Kinnison, J. S. Francisco, A. Saiz-Lopez, D. Roca-Sanjuán, *Angew. Chem. Int. Ed.* **2020**, *59*, 7605–7610; *Angew. Chem.* **2020**, *132*, 7675–7680.
- [35] J. Carmona-García, A. Francés-Monerris, C. A. Cuevas, T. Trabelsi, A. Saiz-Lopez, J. S. Francisco, D. Roca-Sanjuán, *J. Am. Chem. Soc.* **2021**, *143*, 10836–10841.
- [36] S. Mai, P. Marquetand, L. González, *WIREs Comput. Mol. Sci.* **2018**, *8*, e1370.
- [37] S. Mai, M. Richter, M. Heindl, M. F. S. J. Menger, A. Atkins, M. Ruckebauer, F. Plasser, L. M. Ibele, S. Kropf, M. Opiel, P. Marquetand, L. González, *sharc-md.org* **2019**. Accessed September 22nd, 2021.

Manuscript received: August 24, 2021

Revised manuscript received: September 22, 2021

Accepted manuscript online: September 25, 2021

Version of record online: October 26, 2021